The Astrophysical Journal, 713:1244–1248, 2010 April 20 doi:10.1088/0004-637X/713/2/1244

SUZAKU OBSERVATIONS OF THE BLACK HOLE H1743−322 IN OUTBURST

J. L. Blum[1], J. M. Miller[1], E. Cackett[1,7], K. Yamaoka[2], H. Takahashi[3], J. Raymond[4], C. S. Reynolds[5], and A. C. Fabian[6]
[1] Department of Astronomy, University of Michigan, 500 Church Street, Ann Arbor, MI 48109, USA
[2] Department of Physics and Mathematics, Aoyama Gakuin University, Shibuya, Tokyo, Japan
[3] Department of Physical Science, Hiroshima University, 1-3-1 Kagamiyama, Higashi-Hiroshima, Hiroshima, 739-8526 Japan
[4] Harvard-Smithsonian Center for Astrophysics, 60 Garden Street, Cambridge, MA 02138, USA
[5] Department of Astronomy, University of Maryland, College Park, MD 20742, USA
[6] University of Cambridge, Institute of Astronomy, Madingley Road, Cambridge CB3 0HA, UK
Received 2009 September 8; accepted 2010 March 3; published 2010 April 1

ABSTRACT

We observed the Galactic black hole candidate H1743−322 with *Suzaku* for approximately 32 ks, while the source was in a low/hard state during its 2008 outburst. We collected and analyzed the data with the HXD/PIN, HXD/GSO, and XIS cameras spanning the energy range 0.7–200 keV. Fits to the spectra with simple models fail to detect narrow Fe XXV and Fe XXVI absorption lines, with 90% confidence upper limits of 3.5 and 2.5 eV on the equivalent width, respectively. These limits are commensurate with those in the very high state, but are well below the equivalent widths of lines detected in the high/soft state, *suggesting that disk winds are partially state-dependent*. We discuss these results in the context of previous detections of ionized Fe absorption lines in H1743−322 and connections to winds and jets in accreting systems. Additionally, we report the possible detection of disk reflection features, including an Fe K emission line.

Key words: accretion, accretion disks – black hole physics – stars: individual (H1743−322) – X-rays: binaries

1. INTRODUCTION

H1743−322 was discovered during its 1977–1978 outburst with the *High Energy Astronomical Observatory-1 (HEAO-1)* and *Ariel 5* (Doxsey et al. 1977; Kaluzienski & Holt 1977). Based on its spectral characteristics, H1743−322 was classified as a Galactic X-ray transient by White & Marshall (1984). The 2003 outburst of H1743−322 allowed for two discoveries that provided evidence that this source harbors a black hole primary. First, Homan et al. (2003) reported the detection of quasi-periodic oscillations at 160 Hz and 240 Hz, a 2:3 frequency ratio that is typical for black hole candidates (e.g., GRO J1655−40: Strohmayer 2001a; GRS 1915+105: Strohmayer 2001b; and XTE J1550−564: Miller et al. 2001). Second, Rupen et al. (2003; see also Corbel et al. 2005) reported a relativistic jet ($v/c \simeq 0.8$) in H1743−322, which allows this source to be termed a "microquasar."

Disk-jet coupling, i.e., the relation between inflow and outflow, has become one of the richest areas of X-ray binary research. The "low/hard" and the "high/soft" states are the two most diametrically opposed in regards to jet formation. The low/hard state is characterized by an energy spectrum that is dominated by a power-law-like component. A photon index of ∼1.6 and a high-energy cutoff at ∼100 keV (Fender & Belloni 2004) are typical for a black hole X-ray binary in the low/hard state. A weak soft X-ray component, most likely associated with a thermal disk (e.g., Miller et al. 2006a; Reis et al. 2009), can also be present. In contrast, a strong thermal component, which can be modeled as a disk-blackbody with an inner temperature of 1–2 keV, is prevalent in the high/soft state (Fender & Belloni 2004). When both GRS 1915+105 (Dhawan et al. 2000) and Cyg X-1 (Stirling et al. 2001) were in the low/hard state, Very Long Baseline Interferometry radio images have shown a spatially resolved radio jet during periods of quasi-steady radio and hard X-ray emission. However, in the high/soft state there is a dramatic drop in the radio emission compared to the low/hard state (e.g., Fender & Belloni 2004). Although the nature of radio emission in the "very high state" remains unclear, McClintock & Remillard (2006) suggest that this state is relatively radio quiet. To date, no source has exhibited optically thick radio emission consistent with a jet in the high/soft state.

In this paper, we refer to observations of H1743−322 in the high/soft state and "very high state" made in 2003 (Miller et al. 2006c). "Intermediate" and "very high" (or steep power law) states appear to be quasi-steady states that share some of the characteristics of both the low/hard and high/soft states. The energy spectrum possesses strong thermal *and* power-law components with no apparent high-energy cutoff. The photon index is typically $\geqslant$2.4, which is steeper than the index seen in the low/hard state (McClintock & Remillard 2006). Transitions between the high/soft and low/hard states frequently pass through intervals of these transitional states. While some suggest that the very high state is in itself an "intermediate" state, we acknowledge the very high state as a bona fide state of black hole binaries in accordance with McClintock & Remillard (2006).

A disk wind can be key to understanding the nature of the accretion flow in disk systems (e.g., Proga 2003; Ueda et al. 2009; Ohsuga et al. 2009). Previously, *Chandra* observations of H1743−322 during its 2003 outburst found evidence of an ionized disk wind in the high/soft state, in the form of blueshifted Fe XXV and XXVI absorption lines (Miller et al. 2006c). Figure 1 compares the light curves of H1743−322 when it was observed in the high/soft state and the low/hard state. The apparent difference in counts per second and hardness between the two states emphasize the distinction between spectral states for black hole binaries. Iron absorption lines were absent when *Chandra* observed H1743−322 in the very high state. Similar results were obtained from *Chandra* observations of GRO J1655−40 (Miller et al. 2006b, 2008) and GRS 1915+105 (Miller et al. 2008; Neilson & Lee 2009). The physical mechanism needed to produce such a disk wind is still being investigated, aided by an extensive theoretical framework

[7] Chandra Fellow.

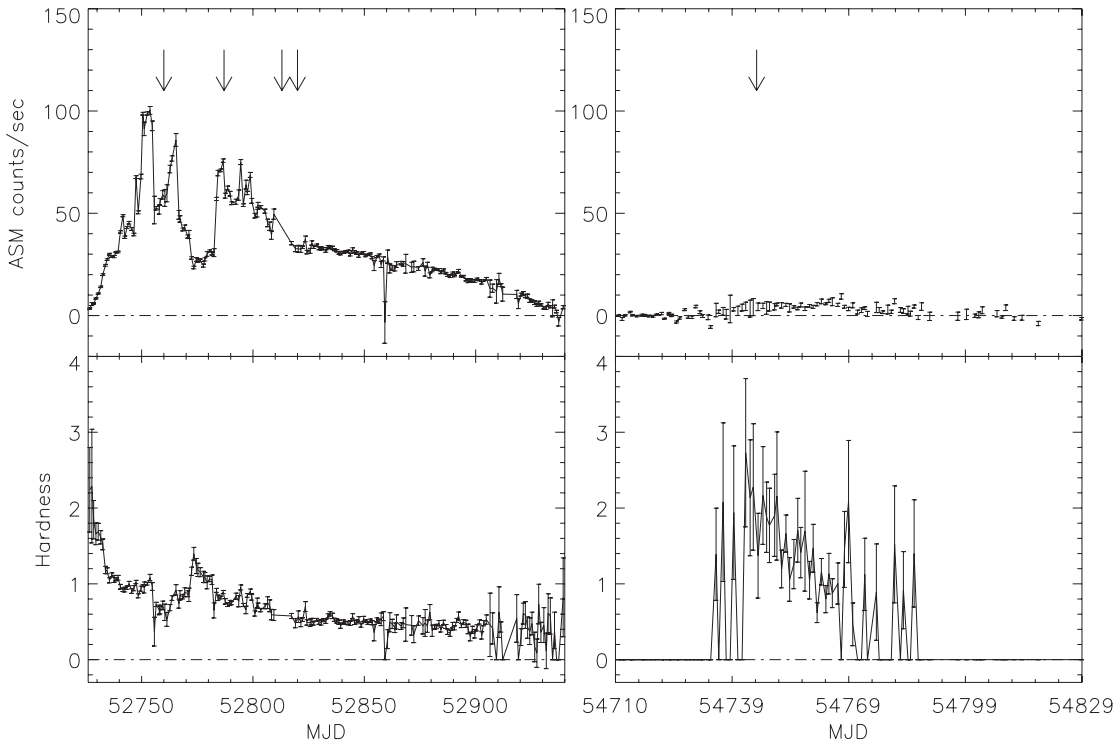

Figure 1. Left panel: *RXTE*/*ASM* one-day averaged light curve with errors (1.5–12 keV) and one-day averaged (5–12 keV)/(3–5 keV) hardness ratio, for the bright phase of the 2003 outburst of H1743−322 (Miller et al. 2006c). The source progresses through the very high or steep power-law state followed by the high/soft state. The arrows at the top of the plot denote the days on which H1743−322 was observed with *Chandra*. Right panel: *RXTE*/*ASM* one-day averaged light curve with errors (1.5–12 keV) and one-day averaged (5–12 keV)/(3–5 keV) hardness ratio, for the 2008 October outburst of H1743−322. The source rise is typical of the low hard state. The arrow at the top of the plot denotes the date on which we observed H1743−322 with *Suzaku*.

(see, e.g., Blandford & Payne 1982; Begelman et al. 1983; Proga et al. 2000). In this paper, we report the results of an analysis of the *Suzaku* X-ray spectra resulting from the H1743−322 2008 October outburst (see Figure 4). Preliminary results from this observation were reported in Blum et al. 2008.

2. DATA REDUCTION

Suzaku observed H1743−322 on 2008 October 7 starting at 16:19:21 (UT). The observation duration was approximately 72 ks. The X-ray Imaging Spectrometer (XIS) pointing position was used. The three detectors constituting the XIS0, XIS1, and XIS3 (energy range 0.2–12 keV) were each operated in 3×3 and 5×5 editing modes; using the 1/4 window mode with a 1.0 s burst option helped to limit photon pileup. No timing mode was used. The energy resolution (FWHM) of the XIS cameras is ∼120 eV at 6.0 keV and ∼50.0 eV at 1.0 keV. Each CCD camera has a single CCD chip with an array of 1024×1024 pixels, and covers an $18' \times 18'$ region on the sky. Each pixel is 24 μm square, and the size of the CCD is 25 mm × 25 mm. The XIS1 sensor uses a back-side illuminated CCD, while the other two use a front-side illuminated CCD (e.g., Koyama et al. 2007). XIS on-source times of approximately 32 ks were achieved. This resulted in a dead-time corrected net exposure of 16 ks for the XIS cameras.

Soft X-ray spectra within the energy ranges 0.7–1.5 keV and 2.2–10.0 keV were used. The 1.5–2.2 keV energy range was ignored to avoid systematic errors due to calibration in the Si band. We used the latest calibration database available at the time of analysis (CALDB 20090925). From the cleaned event files, we extracted the source light curve and spectrum with `xselect`. A circle centered on the source with a radius of 129″ (123 in pixel units) was used for the source extraction region. A circular, off-source region with a radius of 45″ (43 in pixel units) was used to extract the background. The 3×3 and 5×5 mode event files for each XIS detector were loaded together into `xselect`. A single source and background spectrum was extracted from these event files for each XIS detector. The XIS redistribution matrix files (RMFs) and ancillary response files (ARFs) were created using the tools `xisrmfgen` and `xissimarfgen` available in the HEASOFT version 6.6.2 data reduction package. The 3×3 and 5×5 mode event files were used to specify good time intervals and the data was grouped to a minimum of 300 counts per bin using the FTOOL `grppha`.

The Hard X-ray Detector (HXD) covers the energy range 10.0–700 keV and is a combination of Positive Intrinsic Negative (PIN) silicon diodes and Gadolinium Silicate (GSO) phoswich counters. A net exposure of 29 ks was achieved using the HXD (PIN and GSO) cameras, which were operated in their normal mode. The HXD features an effective area of ∼160 cm^2 at 20.0 keV and ∼260 cm^2 at 100 keV (e.g., Takahashi et al. 2007). The HXD time resolution is 61 μs. The HXD-PIN/GSO data were reprocessed from an unscreened event file with up-to-date calibration databases in accordance with the *Suzaku* Data Reduction Guide (CALDB 20090511). The appropriate response matrices for the XIS aim point and background files were downloaded from the *Suzaku* Web page. In our analysis, the energy range for the HXD cameras was restricted to 12.0–200 keV.

3. DATA ANALYSIS AND RESULTS

Using the X-ray spectral fitting software package (XSPEC v. 11.3.2; Arnaud 1996), the *Suzaku* H1743−322 spectra from the three XIS detectors and the HXD detector were fit jointly. A normalizing constant (ranging between 1.0 and 1.1) was allowed

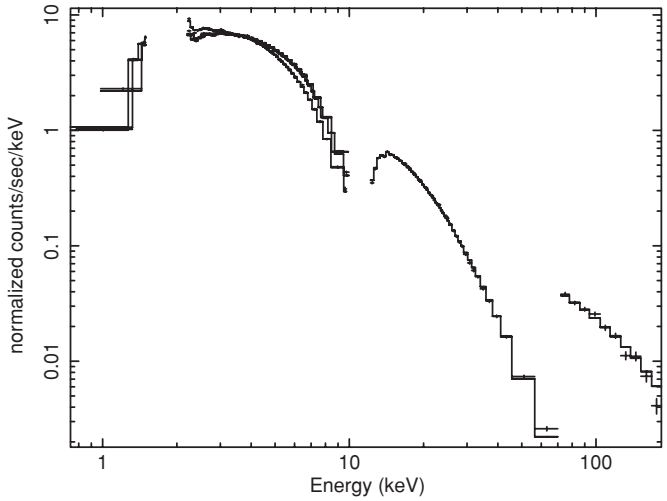

Figure 2. *Suzaku* spectrum of H1743−322 fitted with a broken power-law model (see Table 1). The curves within the 0.7–1.5 keV and 2.2–10.0 keV energy ranges represent the data from the XIS detectors. The curves within the 12.0–70.0 keV and 70.0–200 keV energy ranges represent the data from the PIN and GSO detectors, respectively.

Table 1
Broken Power-law Model Parameters

Parameter	Value
$N_{\rm H}(10^{22}$ cm$^{-2})$	2.00(1)
Γ_1	1.55(1)
Γ_2	2.2(1)
$E_{\rm break}$(keV)	36(2)
$K_{\rm bnpl}$	0.280(3)
$F_{0.5-200}(10^{-9})$	7.51(8)
$L_{\rm X}(0.5–200)(10^{37}$ erg s$^{-1})$	6.37(7)
χ^2/ν	3053/3093

Notes. The results of a broadband spectral fit to the *Suzaku* spectra in the 0.7–200 keV band are presented above. The model is described in XSPEC as `tbabs` × (`bknpow`). A constant was allowed to float between the XIS, PIN, and GSO data. The normalization of the broken power-law component is photons cm^{-2} s^{-1} keV^{-1} at 1 keV. The flux quoted above is an "unabsorbed" flux. The distance to H1743−322 is unknown; a Galactic center distance of d = 8.5 kpc was assumed to calculate the luminosity value. All errors are 90% confidence errors. Errors given in parentheses are symmetric errors in the last significant digit.

to float between spectra to account for different detector flux zero-points. Our initial spectral model consisted of an absorbed power law ($\chi^2/\nu = 3348/3095$). We used `tbabs` in our model to account for photoelectric absorption in the interstellar medium (ISM). Replacing a simple power law with a broken power law provided an improved fit ($\chi^2/\nu = 3053/3093$) with $E_{\rm break} \simeq 36(2)$ keV, $\Gamma_1 \simeq 1.55(1)$, and $\Gamma_2 \simeq 2.2(1)$.

The fit results in the 0.7–200 keV band with the absorbed broken power-law model are reported in Table 1 with a spectral fit being shown in Figures 2–3. For Figure 3, we note that the residuals near 10.0 keV in the XIS spectra are likely due to calibration uncertainties and not photon pile-up (different size extraction regions had negligible effect on the resulting spectral fit). The spectral parameters obtained through our fits for H1743−322 are typical of a Galactic black hole candidate in the low/hard state (McClintock & Remillard 2006; Fender & Belloni 2004). Note that the high equivalent neutral hydrogen column density ($2.00(1) \times 10^{22}$ cm^{-2}) along the line of sight is

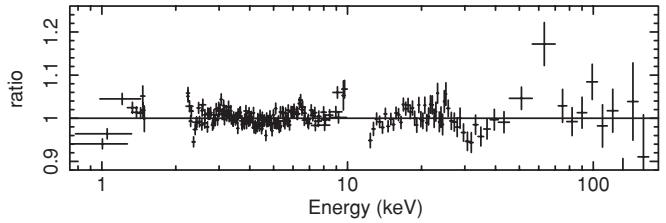

Figure 3. Data/model ratio for the broken power-law model. The curves within the 0.7–1.5 keV and 2.2–10.0 keV energy ranges represent the data from the XIS detectors. The curves within the 12.0–70.0 keV and 70.0–200 keV energy ranges represent the data from the PIN and GSO detectors, respectively.

Table 2
Comptonization Model Parameters

Parameter	Value
$N_{\rm H}(10^{22}$ cm$^{-2})$	1.98(1)
$T_{\rm o}$(keV)	0.25(2)
$T_{\rm e}$(keV)	38(5)
τ	1.6(2)
Normalization($\times 10^{-2}$)	1.9(2)
χ^2/ν	3066/3092

Notes. The results of a broadband spectral fit to the *Suzaku* spectra in the 0.7–200 keV band are presented above. The model is described in XSPEC as `tbabs` × (`compTT`). A constant was allowed to float between the XIS, PIN, and GSO data. The redshift was set to zero and disk geometry was assumed. Errors given in parentheses are symmetric errors in the last significant digit.

consistent with a central Galactic distance to H1743−322 and is in accordance with the value used by Miller et al. (2006c). The unabsorbed flux inferred in the 0.5–200 keV band is $(7.51 \pm 0.08) \times 10^{-9}$ erg cm^{-2}s^{-1}. Currently, the mass of H1743−322 and the distance to the source are unknown. But, given its position near the Galactic center ($l \simeq 357.^{\circ}255$, $b \simeq -1.^{\circ}833$) and relatively high column density, it is reasonable to use a Galactic center distance of 8.5 kpc. Using this value as an estimate of the distance to the source gives a luminosity of $L_{\rm X} = (6.37 \pm 0.07) \times 10^{37}\,(d/8.5\ {\rm kpc})^2$ erg s^{-1} (we calculated the Galactic ridge X-ray emission contribution to be negligible and accounted for by our background spectrum). This calculated luminosity indicates that the source would be 0.08 $L_{\rm EDD}$ for a 6 $M_{\odot}$ black hole and 0.05 $L_{\rm EDD}$ for a 10 $M_{\odot}$ black hole.

A broken power law may be a phenomenological description of Compton upscattering of disk photons by a central, hot, electron-dominated "corona" (see, e.g., Ross et al. 1999). Therefore, we also fit a Comptonization model (`compTT`; Titarchuk 1994) to the broadband *Suzaku* data. This is an analytic model describing Comptonization of soft photons in a hot plasma. The approximations used in the model work well for both the optically thin and thick regimes. Fitting the `compTT` model resulted in an electron temperature of kT $\simeq$ 38(5) keV for a disk temperature of kT $\simeq$ 0.25(2) keV (typical disk temperature for the low/hard state; see, e.g., Miller et al. 2006a). The reduced χ^2 for this Comptonization model was $\simeq$3066/3092 (see Table 2). Note that the energy break in our best-fit broken power-law model, which can indicate the electron temperature of the purported corona, is consistent with the electron temperature in the Comptonization model.

To test the presence of the X-ray Fe XXV and Fe XXVI absorption lines in the *Suzaku* spectrum for H1743−322, we added a Gaussian component to the broken power-law continuum model. We froze the line energy at the theoretical values for Fe XXV

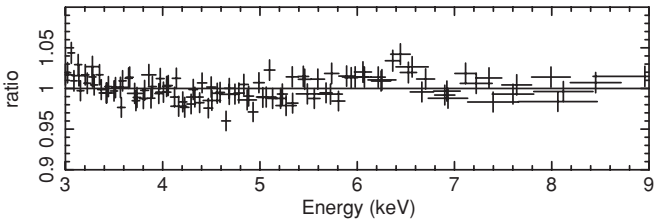

Figure 4. Data/model ratio from 3–9 keV for the broken power-law model. The curves represent the data from the XIS detectors. There is a possible emission line around 6.4 keV.

Table 3
X-ray Absorption Lines Upper Limits

Parameter	Theoretical Value (Å)	Flux (10^{-5} photons cm^{-2} s^{-1})	W (mÅ, eV)
Fe XXV	1.850	5.1	0.97, 3.5
Fe XXVI	1.780	3.4	0.64, 2.5

Notes. Parameters for the He-like Fe XXV ($1s^2$–$1s2p$) and H-like Fe XXVI ($1s$–$2p$) resonance absorption lines. Since no significant lines were detected, 90% confidence upper limits are given.

(6.70 keV) and Fe XXVI (6.97 keV), respectively. The line width was frozen at zero (due to the likelihood that the lines would be at least as narrow as those observed with *Chandra*; see Miller et al. 2006c), while the line flux normalization parameter (in units of photons cm^{-2}s^{-1}) was allowed to vary. Error analysis was performed on the line flux (using the `error` command) to derive the maximum allowable iron line normalization at 90% confidence. The line wavelengths, fluxes, and equivalent widths are listed in Table 3. The equivalent width upper limits for both iron absorption lines were <3.5 eV.

Based on these results, we conclude that these iron absorption lines were not present in the *Suzaku* spectrum for H1743−322 when it was observed in the low/hard state. The Miller et al. (2006c) *Chandra* observations spanned several black hole binary spectral states, particularly the very high state and the high/soft state. Similar to our *Suzaku* results, the Fe XXV and Fe XXVI absorption lines were absent in the source's spectrum in the very high state (equivalent width upper limits <4.3 eV; see Miller et al. 2006c). For softer states (i.e., the high/soft state), however, each detection of Fe XXV and Fe XXVI absorption lines was at the 4σ level of confidence or higher (with, e.g., equivalent widths of 16(1) eV and 25(3) eV, respectively; see Miller et al. 2006c, their Table 3). The combined results of *Suzaku* and *Chandra* indicate that there is a spectral state dependence on absorption lines, and therefore disk winds.

Disk reflection features are common amongst Galactic black hole X-ray spectra (Miller 2007). As shown in Figure 4, there is a potential Fe Kα emission line present in the *Suzaku* spectra. A Gaussian component was added to the broken power-law model to get estimates on the strength of possible Fe Kα emission lines. The 90% confidence levels on the strength of narrow and/or broad Fe Kα emission lines are given in Table 4 for line energy and FWHM values. The line energy and width were allowed to vary from 6–7 to 0–3.0 keV, respectively, for the low ionization iron parameter. This resulted in a low equivalent width of 17(6) eV and a line flux of 0.3(1) (10^{-5}) photons cm^{-2} s^{-1} with FWHM = 0.6(3) keV. A weak Fe K emission line in the *Suzaku* spectra (see Figure 3) of H1743−322 is statistically significant, though the line has an equivalent width of just 17(6) eV (F-value > 8.0, making the line significant at more than the 4.0σ level of confidence). Note that for low ionization iron (Fe I–Fe XVI), a theoretical line energy of 6.40 keV can reasonably be taken to probe Fe I–Fe XVI since the line energy changes only 0.03 keV between those charge states (Kallman et al. 2004). Also note that we made broadband reflection fits to the spectra. For consistency, we investigated models for a relativistic line profile around a rotating black hole convolved with a broken power law reflected from ionized matter (specifically, `tbabs × (laor + kdblur × bexriv)`; see Laor 1991; Magdziarz & Zdziarski 1995). However, these models were poorly constrained and were not statistically superior to the broken power law and thermal Comptonization models.

4. DISCUSSION

We have analyzed a sensitive *Suzaku* observation of the Galactic black hole candidate H1743−322 in the low/hard state. The continuum spectrum can be described using a broken power law or thermal Comptonization. The spectrum is interesting for lacking evidence of an X-ray disk wind. When combined with prior results, our findings suggest that disk winds are partially state-dependent. There is also weak evidence for a neutral Fe K emission line, which likely arises in the disk.

Previous observations show that disk winds in stellar-mass black holes seem to be stronger in soft disk-dominated (high/soft) states than in other states (e.g., Miller et al. 2006c, 2008; Neilson & Lee 2009). Indeed, it is possible that winds and jets are anti-correlated (Miller et al. 2006c, 2008; Neilson & Lee 2009)—the disk may alternate its outflow mode. In GRS 1915+105, Miller et al. (2008) and Neilson & Lee (2009) found broad He-like Fe XXV emission lines in the low/hard state and highly ionized narrow H-like Fe XXVI lines in the high/soft state. Equivalent widths ranged ∼5–30 eV for the H-like Fe XXVI absorption lines (Neilson & Lee 2009, their Table 1), which are consistent with those observed in the high/soft state *Chandra* observation for H1743−322 (Miller et al. 2006c). Ueda et al. (2009) also detected both H-like Fe XXVI and He-like Fe XXV absorption lines (with equivalent widths of ∼40 eV) in the high/soft state for GRS 1915+105. While both sources differ in subtle ways from the "canonical" spectral states for X-ray binaries (GRS 1915+105: see Belloni et al. 2000; H1743−322: see Homan et al. 2005), the prevalence of disk winds in the high/soft state is clear.

Table 4
X-ray Emission Line Detection

Parameter	Theoretical Value (Å, keV)	Model Value (keV)	FWHM (keV)	Flux (10^{-5} photons cm^{-2} s^{-1})	W (mÅ, eV)
Low ion. Fe	1.940, 6.40	6.3(1)	0.6(3)	0.3(1)	5(2), 17(6)

Notes. Parameters for low ionization iron (Fe I–Fe XVI), He-like Fe XXV, and H-like Fe XXVI emission lines for the `tbabs × (gaussian + bknpow)` model. 90% confidence errors are given. Low ionization iron with FWHM = 0.6 keV is a weak detection that resulted from allowing the line energy to vary between 6 and 7 keV while σ varied between 0 and 3 keV. Note that the line energy for low ionization iron changes only 0.3 keV between those charge states, which is the reason 6.40 keV was used as the theoretical value.

Miller et al. (2006c) detected absorption lines when *Chandra* observed H1743−322 when it was in the high/soft state (see Homan et al. 2005; Miller et al. 2006c). The Fe XXVI line had a velocity width (FWHM) of $1900 \pm 500\,\mathrm{km\,s^{-1}}$, suggesting a highly ionized medium in outflow. The equivalent widths observed in the high/soft state for Fe XXV and Fe XXVI absorption lines are greater than those we observe in the low/hard state by a factor of approximately 4.4 and 10, respectively. However, those lines were absent in the very high state, with tight upper limits on the line flux. Based on these observations, it was not certain whether the wind was quenched in the very high state, or if the ionization parameter in the wind had merely increased and hindered its detection. In the low/hard state we observed, the 9.0–20.0 keV ionizing flux is a factor of 2.3 lower than in the very high state (Miller et al. 2006c), yet ionized Fe XXV and Fe XXVI absorption lines are ruled out with more stringent upper limits. This demonstrates that disk winds are indeed state-dependent—strongest in the disk-dominated high/soft state, and weak or absent in other states. Furthermore, the lack of a disk wind in the hard state for the 2008 outburst and the detection of relativistic jets in the hard state during the 2003 outburst for H1743−322 (Corbel et al. 2005) support the notion that the disk winds and jets are anti-correlated.

Disk reflection features are common in a majority of Galactic black holes' spectra in the low/hard state (e.g., Rossi et al. 2005; Miller et al. 2006a). Our analysis of H1743−322 indicates the presence of such features, most notably, the Fe Kα emission line. The predicted equivalent widths of the Fe K emission line depend on the geometry, inclination, and ionization state of the system. For a centrally illuminated neutral disk with varying power-law photon index ($1.3 \leqslant \Gamma \leqslant 2.3$), an equivalent width between 100 and 150 eV is expected for an inclination range of 45°–60° (George & Fabian 1991, their Figure 14). For an ionized disk ($1.0 < \log \xi < 5.0$, with ξ being the ionization parameter), equivalent widths can range between 100 and 500 eV (Ballantyne et al. 2002: Figure 3). Note that Miller et al. (2006c) detected no reflection features for this source in the high/soft state and the very high state. Based on the calculations in George & Fabian (1991), a possible explanation for our low equivalent width values is a high inclination (i.e. $\theta > 80°$). Viewing the central engine through a corona seen at high inclination can serve to diminish the clarity of reflection features (Petrucci et al. 2001). Dips seen in the light curves for H1743−322 also indicate that the source is likely viewed at a high inclination (Miller et al. 2006c: Figure 5).

Additionally, by using the width (i.e., FWHM) of the Fe K emission line, we can estimate how far the inner disk extends in H1743−322. Note that there is high uncertainty in FWHM (0.6(3) keV), which only allows for lower and upper boundaries of the inner disk radius. Based on our model (i.e., broken power law added to a Gaussian component) and given in units of gravitational radii ($r_g = GM_{\mathrm{BH}}/c^2$), the inner disk ranges from ∼40–600 r_g. The innermost stable circular orbit (ISCO) around a nonspinning black hole is $r_{\mathrm{ISCO}} = 6\,r_g$. A possible explanation for the large differences between our estimates and the expected inner disk radius for a nonspinning black hole is that the inner disk does not extend to the ISCO and is truncated (see, e.g., Esin et al. 1997). However, given that our estimates are inferred from parameter values that are poorly constrained, we must regard our inferred radii with caution. It is possible, for instance, that the detection of a red wing in a relativistic line is prevented by calibration uncertainties in the 2.0–3.0 keV band, which can have a small impact on the continuum.

Although examining disk winds and disk reflection in stellar-mass black holes can be observationally challenging, the possibility of a state-dependent anti-correlation between winds and jets may offer insights into different active galactic nucleus modes (i.e., radio-loud versus radio-quiet). *Chandra*, *XMM-Newton*, and *Suzaku* all can make important contributions in this regard. In the near future, *Astro-H* and the *International X-ray Observatory* will be able to study winds and reflection in unprecedented detail using microcalorimeter spectrometers.

We thank the *Suzaku* mission managers for executing our requested observations. We acknowledge helpful conversations with Koji Mukai.

REFERENCES

Arnaud, K. A. 1996, in ASP Conf. Ser. 101, Astronomical Data Analysis Software and Systems V, ed. G. H. Jacoby & J. Barnes (San Francisco, CA: ASP), 17
Ballantyne, D. R., Fabian, A. C., & Ross, R. R. 2002, MNRAS, 329, L67
Begelman, M. C., McKee, C. F., & Shields, G. A. 1983, ApJ, 271, 70
Belloni, T., Klein-Wolt, M., Méndez, M., van der Klis, M., & van Paradijs, J. 2000, A&A, 355, 271
Blandford, R. D., & Payne, D. G. 1982, MNRAS, 199, 883
Blum, J. L., et al. 2008, ATel, 1841, 1
Corbel, S., Kaaret, P., Fender, R. P., Tzioumis, A. K., Tomsick, J. A., & Orosz, J. A. 2005, ApJ, 632, 504
Dhawan, V., Mirable, I. F., & Rodríguez, L. F. 2000, ApJ, 543, 373
Doxsey, R., et al. 1977, IAU Circ., 3113, 2
Esin, A., McClintock, J., & Narayan, R. 1997, ApJ, 498, 865
Fender, R., & Belloni, T. 2004, ARA&A, 42, 317
George, I. M., & Fabian, A. C. 1991, MNRAS, 249, 352
Homan, J., Klein-Wolt, M., Rossi, S., Miller, J. M., Wijnands, R., Belloni, T., van der Klis, M., & Lwein, W. H. G. 2003, ApJ, 586, 1262
Homan, K., Miller, J. M., Wijnands, R., van der Klis, M., Belloni, T., Steeghs, D., & Lewin, W. H. G. 2005, ApJ, 623, 383
Kallman, T. R., Palmeri, P., Bautista, M. A., Mendoza, C., & Krolik, J. H. 2004, ApJS, 155, 675
Kaluzienski, L. J., & Holt, S. S. 1977, IAU Circ., 3099, 3
Koyama, K., et al. 2007, PASJ, 59, S23
Laor, A. 1991, ApJ, 376, 90
Magdziarz, P., & Zdziarski, A. A. 1995, MNRAS, 273, 837
McClintock, J. E., & Remillard, R. A. 2006, in Compact Stellar X-ray Sources, ed. W. Lewin & M. van der Klis (Cambridge: Cambridge Univ. Press), 157
Miller, J. M. 2007, ARA&A, 45, 441
Miller, J. M., Homan, J., Steeghs, D., Rupen, M., Hunstead, R. W., Wijnands, R., Charles, P. A., & Fabian, A. C. 2006a, ApJ, 653, 525
Miller, J. M., Raymond, J., Fabian, A., Steeghs, D., Homan, J., Reynolds, C., van der Klis, M., & Wijnands, R. 2006b, Nature, 441, 953
Miller, J. M., Raymond, J., Reynolds, C. S., Fabian, A. C., Kallman, T. R., & Homan, J. 2008, ApJ, 680, 1359
Miller, J. M., et al. 2001, ApJ, 563, 928
Miller, J. M., et al. 2006c, ApJ, 646, 394
Neilson, J., & Lee, J. C. 2009, Nature, 458, 481
Ohsuga, K., Mineshige, S., Mori, M., & Kato, Y. 2009, PASJ, 61, 7
Petrucci, P. O., Merloni, A., Fabian, A., Haardt, F., & Gallo, E. 2001, MNRAS, 328, 501
Proga, D. 2003, ApJ, 585, 406
Proga, D., Stone, J. M., & Kallman, T. R. 2000, ApJ, 543, 686
Reis, R. C., Miller, J. M., & Fabian, A. C. 2009, MNRAS, 395, L52
Ross, R. R., Fabian, A. C., & Young, A. J. 1999, MNRAS, 306, 461
Rossi, S., Homan, J., Miller, J. M., & Belloni, T. 2005, MNRAS, 360, 763
Rupen, M. P., Mioduszewski, A. J., & Dhawan, V. 2003, ATel, 139, 1
Stirling, A. M., Spencer, R. E., de la Force, C. J., Garrett, M. A., Fender, R. P., & Ogley, R. N. 2001, MNRAS, 327, 1273
Strohmayer, T. E. 2001a, ApJ, 552, L49
Strohmayer, T. E. 2001b, ApJ, 554, L169
Takahashi, T., et al. 2007, PASJ, 59, 35
Titarchuk, L. 1994, ApJ, 434, 570
Ueda, Y., Yamaoka, K., & Remillard, R. 2009, ApJ, 695, 888
White, N. E., & Marshall, F. E. 1984, ApJ, 281, 354